Macrophage PPARγ, a lipid activated transcription factor controls a growth factor GDF3 and skeletal muscle regeneration

Tamas Varga[#1], **Rémi Mounier**[#2], **Andreas Patsalos**[1], **Péter Gogolák**[3], **Matthew Peloquin**[4], **Attila Horvath**[1], **Attila Pap**[1], **Bence Daniel**[1,4], **Gergely Nagy**[1,5], **Eva Pintye**[6], **Szilárd Póliska**[1], **Sylvain Cuvellier**[7], **Sabrina Ben Larbi**[2], **Brian E. Sansbury**[8], **Matthew Spite**[8], **Chester W. Brown**[9,10,11], **Bénédicte Chazaud**[2,7,*], and **Laszlo Nagy**[1,4,5,*]

[1] Department of Biochemistry and Molecular Biology, University of Debrecen, Debrecen, H-4012, Hungary

[2] Institut NeuroMyogène, INMG, Université Claude Bernard Lyon 1, CNRS UMR5310, Villeurbanne 69100, INSERM U1217, France

[3] Department of Immunology, University of Debrecen, Debrecen, H-4012, Hungary

[4] Sanford-Burnham-Prebys Medical Discovery Institute at Lake Nona, 6400 Sanger Road, Orlando, FL 32827

[5] MTA-DE "Lendület" Immunogenomics Research Group, University of Debrecen, Debrecen, H-4012, Hungary

[6] Department of Radiation Therapy, University of Debrecen, Debrecen, H-4012, Hungary

[7] Institut Cochin, INSERM U1016, CNRS, UMR8104, Université Paris Descartes, Sorbonne Paris Cité, Paris 75014, France

[8] Center for Experimental Therapeutics & Reperfusion Injury, Department of Anesthesiology, Perioperative and Pain Medicine, Brigham and Women's Hospital, Harvard Medical School, Boston, MA, 02115

[9] Department of Molecular and Human Genetics, Baylor College of Medicine, Houston, TX 77030

[*] Corresponding authors: Laszlo Nagy (Lead Contact), lnagy@sbpdiscovery.org, phone: +1-407-745-2150, Bénédicte Chazaud, benedicte.chazaud@inserm.fr, phone: +33-4-72431051.

[10] Department of Pediatrics, Baylor College of Medicine, One Baylor Plaza, Houston, TX 77030

[11] Texas Children's Hospital, Houston, TX 77030

[#] These authors contributed equally to this work.

SUMMARY

Tissue regeneration requires inflammatory and reparatory activity of macrophages. Macrophages detect and eliminate the damaged tissue and subsequently promote regeneration. This dichotomy requires the switch of effector functions of macrophages coordinated with other cell types inside the injured tissue. The gene regulatory events supporting the sensory and effector functions of macrophages involved in tissue repair are not well understood. Here we show that the lipid activated transcription factor, PPARγ, is required for proper skeletal muscle regeneration, acting in repair macrophages. PPARγ controls the expression of the transforming growth factor-β (TGF-β) family member, GDF3, which in turn regulates the restoration of skeletal muscle integrity by promoting muscle progenitor cell fusion. This work establishes PPARγ as a required metabolic sensor and transcriptional regulator of repair macrophages. Moreover, this work also establishes GDF3 as a secreted extrinsic effector protein acting on myoblasts and serving as an exclusively macrophage-derived regeneration factor in tissue repair.

Graphical Abstract

Ly6C- macrophages at Day 4
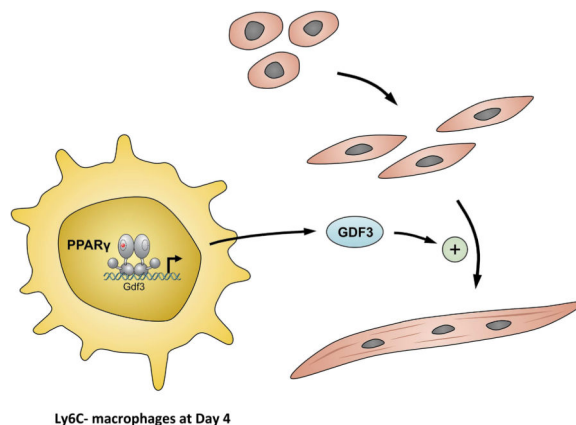
INTRODUCTION

Tissues suffer damage during an organism's lifetime. In order to maintain the body's integrity and homeostasis, it is critically important to achieve complete regeneration. In many cases a straightforward paradigm can be applied whereby organ injury induces expansion and differentiation of a quiescent population of tissue-specific stem cell-like progenitors. Impaired injury-related immune response has been shown to greatly influence regeneration in liver, central nervous system or skeletal muscle (Chazaud, 2014; Duffield et al., 2005; Laflamme and Murry, 2011; Rapalino et al., 1998). Immune cells and in particular, macrophages sense the injury, remove damaged tissues, then initiate restoration of tissue integrity *via* promoting repair mechanisms. During this latter phase the immune response regulates the reengagement of tissue progenitor cell populations to support cell growth and

differentiation. Our knowledge is fragmented on how macrophages employ sensory and regulatory mechanisms and use effector functions to serve their reparatory roles. We sought to identify such integrated regulatory mechanisms that equip a macrophage with the capacity to contribute to a timely progression of repair.

We found that the fatty acid regulated transcription factor, Peroxisome Proliferator-Activated Receptor gamma (PPARγ) (Tontonoz et al., 1998), was required in repair macrophages during skeletal muscle regeneration. Mice with a deletion of PPARγ in their myeloid lineages showed a pronounced delay in regeneration. PPARγ regulated the expression of a secreted factor, GDF3 in repair macrophages. GDF3 deficiency impaired muscle regeneration and recombinant GDF3 enhanced repair *in vivo* and the fusion of primary myogenic precursor cells (MPCs) in *in vitro* cultures. Our data reveal a PPARγ-GDF3 pathway with sensory, gene regulatory and effector components in which PPARγ in repair macrophages responds to signals and support the timely promotion of tissue repair during skeletal muscle regeneration.

RESULTS

PPARγ is expressed in macrophages of the cardiotoxin induced skeletal muscle injury model

Skeletal muscle possesses robust regenerative capacity, therefore it provides us with an excellent model system to study regeneration. The best characterized experimental model of skeletal muscle injury is the toxin induced injury and regeneration. We triggered skeletal muscle damage in the *tibialis anterior* (TA) muscle of mice by intramuscular injection of the snake venom, Cardiotoxin (CTX), to induce a homogenous and synchronous muscle damage that is repaired with the active contribution of infiltrating immune cells. We isolated macrophage populations from injured muscle and interrogated their gene expression profiles by microarray analysis. When the expression profiles of inflammatory Ly6C$^+$ and repair Ly6C$^-$ macrophages derived from injured muscle at day 2 CTX injury were compared, gene ontology (GO) annotation categories belonging to lipid and carbohydrate metabolism dominated the biological processes that were the most robustly upregulated in the Ly6C$^-$ (repair) macrophages (Fig S1A). When analyzing the expression data, we found that a master regulator of metabolism, *Pparg*, was highly expressed in these macrophages. Using publicly available gene expression data within the Immunological Genome Project, we compared the expression of *Pparg* in muscle infiltrative macrophages to that of their direct precursors, Ly6C$^+$ monocytes (Varga et al., 2013), and various other myeloid cells (Fig S1B). We found that *Pparg* in muscle macrophages was highly expressed, and that only two *in vivo* macrophage subtypes, alveolar macrophages and splenic red pulp macrophages expressed *Pparg* higher. In contrast to *Pparg, Ppara* was not expressed in muscle infiltrative macrophages, while the expression of *Ppard* showed a declining expression in the course of regeneration (Fig S1C).

Based on these findings, we hypothesized that macrophage PPARγ is a metabolic sensor and regulator of skeletal muscle regeneration. To test this hypothesis, we used the *Pparg*$^{fl/fl}$ *Lyz2-cre* mouse strain, which is deficient in PPARγ specifically in myeloid lineages (Clausen et al., 1999). When CD45$^+$ cells, which comprise all infiltrating hematopoietic

cells, or sorted macrophages, were isolated from injured skeletal muscle, the expression of *Pparg* was detected in these cells by RT-qPCR (Figs S1D and S1E) in wild type (WT) animals. Furthermore, the expression of *Pparg* was greatly diminished in corresponding CD45$^+$ cells and macrophages isolated from *Pparg*$^{fl/fl}$ *Lyz2-cre* animals, validating the suitability of this genetic model for these experiments.

Macrophage PPARγ regulates skeletal muscle regeneration

Wild Type and *Pparg*$^{fl/fl}$ *Lyz2-cre* animals were injected with CTX to induce TA muscle injury and then regeneration was analyzed by a combination of morphometric and flow cytometry analysis. We found *Pparg*$^{fl/fl}$ *Lyz2-cre* animals showed a pronounced delay in muscle regeneration (Figs 1A-D and S2A). First, the cross-sectional area (CSA) of the regenerating muscle fibers was significantly smaller in the *Pparg*$^{fl/fl}$ *Lyz2-cre* than in WT mice at day 8 and day 21 following CTX injury (Figs 1C and S2A). Second, there were a significantly higher number of phagocytic and/or necrotic fibers present at day 8 post CTX in *Pparg*$^{fl/fl}$ *Lyz2-cre* mice (Figs 1A-B), indicating either a delayed clearance of dying myofibers or an altered dynamics of muscle fiber death in *Pparg*$^{fl/fl}$ *Lyz2-cre* animals. Third, increased inflammatory infiltration persisted in small regions in the regenerative areas in *Pparg*$^{fl/fl}$ *Lyz2-cre* muscles at day 8 (Fig 1A), which were resolved by day 21 (Fig S2B). Next, we wanted to ascertain whether PPARγ deficiency in the hematopoietic compartment was the major contributor to the observed phenotype. To prove this, we used a second genetic model, in which bone marrow from the epiblastic conditional ablation of *Pparg* (*Pparg*$^{fl/-}$, *Sox2-cre*$^+$) (Nadra et al., 2010) or WT animals were used to reconstitute the hematopoietic compartment in irradiated WT animals (bone marrow transplanted or BMT animals). TA muscles of recipient BMT animals were injected with CTX 12 weeks after BMT and histological analysis of muscle regeneration was carried out 22 days post injury. When compared with animals that received WT bone marrow (WT BMT), mice that received bone marrow deficient in PPARγ (*Pparg*$^{fl/-}$, *Sox2-cre*$^+$ BMT) exhibited a profound deficit in regeneration (Figs 1E-F). Further underlying the importance of PPARγ in muscle regeneration, full body *Pparg*$^{fl/-}$ *Sox2-cre*$^+$ animals displayed impairment in their skeletal muscle regeneration (Fig S2C).

PPARγ deficiency does not alter macrophage infiltration or differentiation in injured muscle

Several possible reasons could explain why macrophage PPARγ deficiency leads to such impairment in muscle regeneration. One underlying reason behind our observations could be a decreased macrophage infiltration in *Pparg*$^{fl/fl}$ *Lyz2-cre* animals. To monitor the cellular dynamics of immune infiltration in CTX injured muscle, we treated WT and *Pparg*$^{fl/fl}$ *Lyz2-cre* animals with CTX, then isolated and analyzed immune cells from injured muscles on days 1, 2 or 4, using CD45$^+$ magnetic bead selection. We found no major difference between the numbers and types (Ly6C^{mid} F4/80$^-$ neutrophils, Ly6C$^+$ F4/80^{low} and Ly6C$^-$ F4/80^{high} macrophages) of infiltrating immune cells in WT *vs.* *Pparg*$^{fl/fl}$ *Lyz2-cre* animals (Fig. S3), with the exception of minor alterations in the ratio of neutrophils at day 1 and in the total number of CD45$^+$ cells at day 6.

Next, we wanted to explore which macrophage functions might be relevant to muscle regeneration and regulated by PPARγ activity. To test the possible contribution of impaired phagocytosis, we used bone marrow derived macrophages (BMDMs) isolated from WT, *Pparg*^fl/fl^ *Lyz2-cre* or WT BMT and *Pparg*^fl/−^, *Sox2-cre*^+^ BMT animals (Figs S4A-B). We set up a phagocytosis assay, in which fluorescently labeled necrotic C2C12 myoblasts were co-incubated with BMDMs labeled with a different fluorescent dye. *Pparg*^fl/fl^ *Lyz2-cre* BMDMs showed no significant increase in the number of phagocyting BMDMs or in the amount of phagocytosed substrate as compared with WT BMDMs (Fig. S4B). Similar results were obtained using BMDMs derived from WT BMT or *Pparg*^fl/−^, *Sox2-cre*^+^ BMT animals, except that *Pparg*^fl/−^, *Sox2-cre*^+^ BMT BMDMs were able to phagocytose a greater load. Our results indicated that an inadequate phagocytic clearance was unlikely to be responsible for the observed delay.

Macrophage PPARγ regulates myoblast differentiation in a paracrine manner in vitro

These results led us to test if macrophage PPARγ activity confers a yet unidentified muscle differentiation-promoting phenotype to macrophages, which could explain the observed delayed muscle regeneration in animals deficient in PPARγ in macrophages. To test this hypothesis, we used *in vitro* muscle precursor cell proliferation or differentiation assays that utilize primary myoblasts isolated from WT mice (Figs 2A-B). In the first assay, we cultured primary myoblasts with conditioned medium derived from non-treated, interferon-γ (IFN-γ) or interleukin-4 (IL-4)-treated WT and *Pparg*^fl/fl^ *Lyz2-cre* BMDMs, in conditions favoring cell proliferation and measured the proliferation index by detecting Ki67^+^ cells by immunofluorescence (IF). As expected, conditioned medium derived from IFN-γ-treated WT BMDMs increased myoblast proliferation (Mounier et al., 2013). Conditioned medium from non-treated *Pparg*^fl/fl^ *Lyz2-cre* BMDMs phenocopied the proliferation enhancing effect of inflammatory WT BMDMs on myoblasts (Fig 2A). These results indicate that PPARγ in macrophages modulated an unknown signaling system that could influence myoblast proliferation in a paracrine manner. Next, we tested the effect of BMDM derived conditioned media on the differentiation of myoblasts by counting the number of cell nuclei within freshly formed desmin positive myotubes cultured in differentiation medium (Fig 2B and Fig S4C). As expected, we observed a large increase in differentiation when myoblasts were grown in conditioned medium derived from IL-4-treated WT BMDMs. Importantly, this increased differentiation was abrogated when conditioned medium from IL-4-treated *Pparg*^fl/fl^ *Lyz2-cre* BMDMs was added to differentiating myoblasts. This effect was seen in several, independently isolated primary myoblast cell lines that were used for the experiments (Fig S4C). BMDM supernatant derived from IFN-γ-treated cells, on the other hand, did not alter myoblast differentiation (Fig S4D). Our results raised the possibility that similar PPARγ–dependent paracrine signaling events took place *in situ* during regeneration, where muscle infiltrative macrophages and MPCs might interact to achieve a synchronized and timely regeneration.

PPARγ regulates cell type specific genes in muscle infiltrating macrophages

Next, we set out to identify PPARγ–dependent regulatory circuits that connect macrophages to myotube differentiation in a paracrine manner. As PPARγ is a transcription factor, we presumed that a relevant change in the gene expression in muscle macrophages must shed

light on the regulatory circuit that is abrogated in *Pparg*^{fl/fl} *Lyz2-cre* macrophages. We isolated populations of macrophages from regenerating muscle from WT and *Pparg*^{fl/fl} *Lyz2-cre* animals and analyzed their gene expression profiles by microarrays (Figs 2C-E and S4E-F). We selected inflammatory Ly6C$^+$ macrophages at day 1 and 2, and repair Ly6C$^-$ macrophages at day 2 and 4 post CTX injury and compared their gene expression by 2 way ANOVA tests (Table S1). We created heat maps for all 4 examined macrophage subsets (Fig 2C). These heatmaps show all genes that were differentially expressed in one relevant subset and also show the expression pattern of these genes in all the other macrophage subsets. The top 5 genes that were most differentially regulated in WT *vs. Pparg*^{fl/fl} *Lyz2-cre* cells are shown in Fig. 2D. The number of genes that were concordantly regulated in a PPARγ–mediated manner in more than one macrophage subtypes is shown in Fig. 2E. We hypothesized those genes could be under regulation by PPARγ that were expressed differently in more than one subtype of muscle macrophages. Accordingly, we combined the lists of upregulated genes reported by the ANOVA analysis of WT *vs. Pparg*^{fl/fl} *Lyz2-cre* comparisons. Although many genes were differentially regulated in a single type of muscle macrophages, only 5 genes (*Saa3*, *Hebp1*, *Plxnd1*, *Apold1*, *Tsg101*) were upregulated in all 4 investigated subtypes of PPARγ deficient muscle macrophages (Fig 2E and table S1). Next, we analyzed the gene sets that were downregulated in *Pparg*^{fl/fl} *Lyz2-cre* macrophages. There was only 1 gene, namely Growth differentiation factor 3 (*Gdf3*), that was consistently downregulated in all 4 investigated macrophage populations (Figs 2D-E). Thus, we identified several putative PPARγ target genes that showed consistent PPARγ dependency in more than one muscle macrophage subsets. To ascertain the PPARγ–dependent regulation of some representative genes, we measured the mRNA expression of *Gdf3*, *Apold1*, *Hebp1* and *Plxnd1* by RT-qPCR in macrophage subsets sorted from injured muscle (Fig S5A). This analysis confirmed the results derived from the microarray experiments. The expression pattern of a short panel of previously described PPARγ-dependent (M2) alternative genes (Odegaard et al., 2007) indicated that the repair macrophages in CTX injured muscles were not canonical M2 macrophages, and that PPARγ exerted little, if any, influence on their expression (Fig S5B). Along the same line, while a total body deficiency in STAT6, the master regulator of IL4 signaling, caused increased presence of phagocytic and/or necrotic fibers at day 8 (Fig S5C), it did not affect the CSA of new myofibers (Fig S5D).

The genes we identified as PPARγ-dependent in muscle macrophages did not belong to the group of canonical PPARγ–regulated genes described in various myeloid cells in earlier studies (such as *Plin2*, *Cd36*, *Angptl4* or *Fabp4*) (Szanto et al., 2010; Welch et al., 2003). One possible reason for this discrepancy could be that most *in vitro* studies apply synthetic or natural ligands of PPARγ to study the transcriptional activity of the receptor upon ligand activation. Therefore, we wanted to see if synthetic PPARγ ligand activation of infiltrating macrophages gave rise to transcriptional changes that are more reminiscent of the list of previously identified PPARγ target genes. For this reason we treated WT animals with rosiglitazone (RSG) *via* gavage and analyzed the ligand dependent gene expression changes in macrophages (Figs S4F and S5E, and Table S1). We found that many more genes were regulated by RSG treatment in Ly6C$^+$ than in Ly6C$^-$ cells. Again, the genes that showed differential expression upon RSG treatment in Ly6C$^+$ cells did not contain established

PPARγ–regulated genes, nor the 6 differently regulated genes that appeared to be under PPARγ regulation in all macrophage subsets. Although RSG treatment caused the differential regulation of fewer genes in Ly6C⁻ cells, the most robustly upregulated gene was *Angptl4*, one of the best-characterized PPARγ target genes. This suggests that not only Ly6C⁻ macrophages at day 2 expressed PPARγ, but that the receptor was also sensitive to the activating effect of an exogenous ligand in Ly6C⁻ cells. It is important to note that *Gdf3*, the gene that was found to be consistently downregulated in *Pparg*^fl/fl *Lyz2-cre* macrophage subsets, was also regulated by RSG treatment (only) in Ly6C⁻ macrophages. Next, we took the list of 43 genes that showed ligand dependent upregulation in Ly6C⁻ macrophages upon RSG treatment and created a heat map representation to see how these genes were regulated in the absence of RSG treatment (Fig S5E). Even without RSG treatment, most of the otherwise RSG dependent genes showed a characteristic induction as Ly6C⁺ macrophages differentiated into Ly6C⁻ cells and an even further induction by day 4. This observation raised the intriguing possibility that the underlying reason behind the limited number of PPARγ ligand regulated genes in Ly6C⁻ macrophages was that most of these genes were already induced during muscle regeneration, even in the absence of exogenous synthetic ligand treatment. Related to this hypothesis, we detected a dynamic *in situ* regulation of eicosanoid synthesis during regeneration. While inflammatory eicosanoids (*e.g.* PGE_2 and $PGF_{2\alpha}$) were detectable in the early inflammatory stages of injury, they were later replaced by lipid mediators produced by murine 12/15-lipoxygenase (*Alox15*) that have been implicated in ligand activation of PPARγ such as 12-HETE and 15-HETE (Fig. S5F) (Huang et al., 1999).

GDF3 is a macrophage-derived PPARγ–dependent member of the TGF-ß family

To focus on putative PPARγ regulated genes whose activity could promote muscle regeneration, we interrogated the list of differently expressed genes for genes that (1) were PPARγ–dependent in more than one macrophage subset, (2) coded a secreted factor and (3) whose activity might be linked to muscle differentiation. Of note, one gene, *Gdf3* (Levine and Brivanlou, 2006; Levine et al., 2009; Shen et al., 2009), fit all these criteria. *Gdf3* was statistically significantly downregulated in *Pparg*^fl/fl *Lyz2-cre* cells in all four investigated macrophage subsets (Figs 2 D-E, Table S1). GDF3 belongs to the TGF-β family, whose members are secreted factors acting in a paracrine manner. Finally, several members of the TGF-β family are known regulators of muscle regeneration, including GDF8 (also known as Myostatin) (McPherron et al., 1997). Therefore, we selected *Gdf3* as the most likely PPARγ–dependent gene that contributes to muscle regeneration for further analysis.

PPARγ occupies a complex set of active enhancers around the Gdf3 locus

Next, we wanted to characterize the genomic events that are responsible for the regulation of *Gdf3* by PPARγ. We elected to use BMDMs, a readily available *in vitro* model system that allowed us to employ high-throughput genomic and epigenomic methods to interrogate the regulatory mechanism exerted by PPARγ on the *Gdf3* locus. We established that WT and *Pparg*^fl/fl*Lyz2-cre* BMDMs provided a platform with good correlation to study the PPARγ–dependent regulation of *Gdf3*, as PPARγ deficiency in BMDMs abrogated the expression of both the canonical PPARγ target gene *Angptl4* and that of *Gdf3* (Fig 3A). Then, we compiled epigenomic and genomic data to identify the relevant enhancers that were active

and possibly under PPARγ regulation in BMDMs (Fig 3B). We included CTCF as a binding factor of insulator regions and RAD21, as a component of the cohesin complex to determine the boundaries of potential chromatin loops or topological domains, PU.1 as a key lineage determining factor in macrophages, RXR (the obligate heterodimeric partner of PPARγ), and PPARγ ChIP-seq data derived from thioglycolate elicited peritoneal macrophages and adipocytes. We combined these data with active epigenetic marks from H3K4me3 ChIP-seq experiments and GRO-seq data from BMDMs. Based on the common CTCF and RAD21 binding sites (Daniel et al., 2014; Merkenschlager and Odom, 2013), the transcription unit of *Gdf3* appeared to be approximately between approximately −50 kb to +50 kb. Our definition of putative, active enhancers included: (1) binding of PU.1, (2) presence of detectable enhancer transcript (GRO-seq signal) (3) RXR or PPARγ binding. This approach was validated by applying the same criteria to the *Angptl4* locus, in which we readily identified its PPARγ–dependent enhancer (Fig S6A). Based on these criteria we nominated 14 putative active enhancers at a distance from +38 Kb to −47 Kb relative to the transcription start site of *Gdf3* (Figs 3B and S6B). As we show in Fig 3C, binding of PPARγ and RXR could be readily detected on 5 of these selected enhancers (at +7.3 kb, −21kb, −25kb, −44kb and −47kb) if we compared WT to *Pparg*^{fl/fl} *Lyz2-cre* BMDMs. These data strongly suggested that *Gdf3* was regulated by one or several of these PPARγ:RXR binding sites.

GDF3 is a regulator of myoblast proliferation, differentiation and muscle regeneration

Next, we analyzed the GDF3 protein expression in whole muscle lysates of CTX injured WT mice, which provided a snapshot of GDF3 protein level during regeneration. The protein expression followed the induction seen at the mRNA level in macrophages and showed a pronounced induction, which peaked at day 4 (Fig 4A), at the time when inflammation subsides and regenerative processes start to dominate within the injured muscle. Importantly, the induction of GDF3 expression was detectable in the CD45^{+} (hematopoietic) compartment and was diminished at both mRNA and protein amount in *Pparg*^{fl/fl} *Lyz2-cre* animals (Figs 4B-D). Next, we further investigated GDF3 expression in alternative models of muscle injuries. We found that, similarly to CTX injury, GDF3 protein expression was induced during glycerol mediated injury and regeneration in WT but diminished in PPARγ macrophage deficient animals (Fig 4E). Furthermore, not only the mRNA expression of *Gdf3*, but the entire panel of genes that showed strong PPARγ dependency in the CTX model, was regulated concordantly in the two models of injury (Fig 4F). GDF3 protein expression was also induced in muscle samples exposed to exposed to crush- and freeze-injuries, which a toxin-free methods (Fig 4G). Due to recent publications that reported a high tendency for false positive detection of GDF proteins in protein detection applications (Egerman et al., 2015), it is important to note that the GDF3 protein induction during CTX injury was undetectable in muscle samples from *Gdf3*^{−/−} animals (Fig 4H). To summarize, GDF3 is a macrophage-derived protein whose expression is induced in various models of muscle regeneration in a PPARγ–dependent manner.

According to our model, the regeneration delay in macrophage PPARγ deficient animals was, at least partly, attributable to a diminished macrophage derived GDF3 secretion within regenerating muscles. This model posits that GDF3 deficiency in macrophages should yield impairment in regeneration comparable to what was observed in *Pparg*^{fl/fl} *Lyz2-cre* animals.

Indeed, muscle regeneration after CTX injury was altered in full body $Gdf3^{-/-}$ animals at day 8 (Figs 5A-B). It has been reported that the full body deletion of $Gdf3$ shows incomplete penetrance (Shen et al., 2009), which suggests possible compensatory mechanisms. To limit their involvement and ascertain the hematopoietic source of GDF3 during muscle regeneration, we generated BMT animals reconstituted with $Gfd3^{-/-}$ BM. When the GDF3 chimeric animals were challenged with CTX induced muscle injury, they exhibited impairment in regeneration at day 16 and 20 (Figs 5C-D). When compared with WT BMT animals, $Gdf3^{-/-}$ chimeras contained more regenerating myofibers with smaller CSA and the regenerating muscle was replete with lipid accumulations, which are hallmarks of defective muscle regeneration (Figs 5C-D). Other cell types, such as fibro-adipogenic progenitors (FAPs) are involved in muscle regeneration (Heredia et al., 2013; Lemos et al., 2015). In line with our results from the $Gdf3^{-/-}$ BMT experiment (Figs 5C-D) and with the mRNA and protein expression data showing GDF3 expression in the $CD45^+$ compartment (Fig 4), $Pdgfra$ expressing FAP cells isolated from D2 regenerating muscle barely expressed $Gdf3$ and $Lyz2$ mRNA (Fig. 5E), rendering the involvement of FAPs unlikely in the macrophage derived GDF3-driven effects on muscle regeneration.

To further prove the requirement for GDF3 in muscle regeneration, we injected recombinant GDF3 into CTX injured muscles of $Pparg^{fl/fl}$ $Lyz2$-cre mice. We found that the exogenously added GDF3 rescued the regeneration deficit seen in these animals (Fig 6A-B). To characterize the function of GDF3 in detail, we cultured primary myoblasts with or without recombinant GDF3. We found GDF3 slightly decreased myoblast proliferation (Fig 6C, left panel). We detected an even more robust effect of GDF3 on myotube formation, as myoblast cultures showed a pronounced increase in their fusion index in the presence of GDF3 (Figs 6C, right panel, and 6D). Myotube formation depends on cell motility, terminal differentiation and cell fusion. In a specific fusion assay, we showed that GDF3 was a potent inducer of myotube formation (Fig S7A), while a differentiation assay indicated that GDF3 did not affect the terminal differentiation of myoblasts into myocytes (Fig S7B).

Next, we investigated if the SMAD2 phosphorylation pathway, which is involved in the signal transduction of several TGF-β superfamily members, is engaged during muscle regeneration. We found a detectable induction of $in\ situ$ pSMAD2 signals in muscles at day 4 of regeneration (Fig 7A), at the time when GDF3 expression peaked in the injured muscle. Furthermore, SMAD2 phosphorylation was significantly increased during $in\ vitro$ treatment of primary myoblasts with GDF3 (Figs 7B-C).

In search for the molecular changes triggered in muscle progenitors in the presence of GDF3, we differentiated $in\ vitro$ primary myoblasts with or without GDF3 and interrogated the gene expression changes by RNA-Seq. First, we compared the profile of primary myoblasts and myoblast-derived myotubes that were cultured in the presence or absence of GDF3. The expression pattern of a preselected list of genes relevant to muscle differentiation (Fig 7D) validated our experimental system. Next, we compared the expression profile of differentiating myotubes cultured with or without GDF3. The list of the differentially regulated genes (Fig 7E and Table S2) showed that a limited set of transcripts were either induced or repressed in the presence of GDF3. Several of the differentially regulated genes, including $Bex1$, (Jiang et al., 2016; Koo et al., 2007), $Sgca$ (Matsumura et al., 1992) and

Camk1g, have been implicated in muscle regeneration, muscle structure and/or Ca^{2+} homeostasis, showing that macrophage derived GDF3 could elicit biologically relevant changes during muscle regeneration.

If GDF3, a macrophage derived secreted factor can regulate *in vitro* and *in situ* muscle differentiation and regeneration, then we wanted to ask if GDF3 is the only macrophage-derived TGF-β family member that is relevant in the context of CTX induced muscle injury. Therefore, we reanalyzed the transcriptomic features of muscle infiltrative macrophages to chart the expression and dynamics of the TGF-β family signaling system (Fig 7F and Fig S7C). Three ligands (*Gdf3*, *Gdf15* and *Inhba*) showed notable gene expression dynamics in muscle infiltrative macrophages. GDF3 expression peaked in repair macrophages and showed definitive, consistent regulation by PPARγ. The two other family members (FigS7C), *Gdf15* and *Inhba*, were also regulated during muscle regeneration, and both genes exhibited partial PPARγ dependency. The PPARγ-GDF3 regulatory axis described in this study therefore identifies a sensory-regulatory-effector mechanism, by which macrophages are regulators of the tissue progenitor compartment, namely MPCs. This axis orchestrates tissue regeneration, possibly in unison with other members of the TGF-β family, leading to synchronous regeneration.

DISCUSSION

Skeletal muscle possesses excellent regenerative capacity, therefore it was striking to see that after CTX injury full body *Pparg*^fl/− *Sox2-cre* animals showed signs of residual inflammation and impaired regeneration. The true extent of the involvement of macrophage PPARγ in the regeneration failure in these animals is unclear for several reasons, including the uncharacterized, but presumably inflammatory state of these animals and the potential involvement of non-macrophage (*e.g.* muscle) PPARγ in regeneration. Therefore we used two distinct genetic models (BMT and conditional PPARγ deficiency, *Pparg*^fl/fl *Lyz2-cre*), which allowed us to focus on the role of PPARγ in macrophages. The delay in regeneration in macrophage PPARγ–deficient animals was less profound than in the epiblastic *Pparg*^−/− mice, yet it was detectable as long as three weeks after the initial injury, thus appearing to be among the most dramatic reported deficiencies in regeneration caused by impairments in macrophage functions (Mounier et al., 2013).

Our analysis did not reveal a gross difference in macrophage number or differentiation in *Pparg*^fl/fl *Lyz2-cre* animals, unlike two other reported experimental systems where AMPK or IGF1 deficiency in muscle infiltrative macrophages led to altered macrophage differentiation (Mounier et al., 2013; Tonkin et al., 2015). Although alternatively activated macrophages have been implicated in tissue repair and PPARγ has been reported to be a regulator of alternative macrophage polarization (Odegaard et al., 2007), we have previously reported that muscle Ly6C^+ and Ly6C^− macrophages do not correspond to canonical alternatively polarized macrophage populations (Varga et al., 2016) in the CTX model. Therefore it is not surprising that, in this model PPARγ is controlling genes other than alternative macrophage related ones, reported to be PPARγ–dependent in other tissue compartments and contexts (Odegaard et al., 2007). The fact that the regeneration impairment in *Stat6*^−/− animals did not manifest in a decrease in CSA, also suggest that PPARγ, in this experimental context,

acts through mechanisms other than modulating alternative macrophage activation. Systematic transcriptomic analyses, however, provided clues about both the sensory and the regulatory roles of PPARγ in muscle infiltrating macrophages. It is important to stress that earlier descriptions of direct PPARγ transcriptional target genes often reported lipid metabolic genes as the main targets PPARγ of in macrophages, which could poorly explain the anti-inflammatory role of the receptor (Szanto et al., 2010; Welch et al., 2003). We report here that the transcriptional activity of PPARγ is unique in muscle macrophages, because the most robustly changing genes (such as *Saa3*, *Hebp1*) were linked to inflammation, rather than to lipid metabolism. Second, *in vivo* treatment with RSG identified the Ly6C$^-$ repair macrophages as an *in situ* macrophage subtype that could be activated by a synthetic ligand for PPARγ. The surprising fact that RSG treatment elicited characteristically different gene expression changes in Ly6C$^+$ and Ly6C$^-$ macrophages isolated from the same tissue and timepoint underscores the notion that distinct macrophage subsets have differential responses to environmental cues. A possible interpretation of the available data would be the involvement of a yet unidentified endogenous ligand for PPARγ whose activity is restricted to the Ly6C$^-$ compartment, which could explain the tendency of otherwise RSG inducible genes to be upregulated in the Ly6C$^-$ macrophages even in the absence of the synthetic ligand. Whether the dynamic regulation of *in situ* eicosanoid synthesis we detected during regeneration could be behind the apparent ligand activation of the receptor, requires further investigation.

From the perspective of muscle regeneration, the most notable finding was the identification of GDF3, a TGF-β family member, which showed consistent regulation by PPARγ in all relevant macrophage subtypes. To ascertain that GDF3 was not only a PPARγ dependent factor, but also a direct PPARγ target, we analyzed an extensive range of genomic and epigenomic data. Although it is clear that GDF3 is expressed in a PPARγ-dependent fashion and can be induced by ligand in muscle derived Ly6C$^-$ macrophages, direct regulation by PPARγ is challenging to prove, because ligand dependent regulation appears to be macrophage subtype specific and not detectable in BMDMs. However, we have provided data that are consistent with direct regulation, even in BMDMs.

It is noteworthy, that both GDF3 gene and protein expressions were much lower in the CD45$^-$ fraction isolated from injured muscle than in the hematopoietic compartment. Considering that the separation of CD45$^+$ cells is inherently incomplete, our results indicate that macrophages are the predominant, if not the only source of GDF3 within the injured tissue. This exclusivity sets GDF3 apart from other macrophage derived regenerative factors, such as IGF1 (Tonkin et al., 2015), which is also produced by muscle and in the liver upon injury. The timing and localization of GDF3 protein in the CTX and other, unrelated injury models firmly suggested that GDF3 is a general, macrophage specific regulator of muscle regeneration.

To link macrophage biology to tissue regeneration, we analyzed the role of macrophage derived GDF3 in muscle regeneration in a combination of *in vivo* and *in vitro* approaches. Foremost, two genetic models of GDF3 deficiency reported a delay in regeneration. While the decrease in average CSA in *Gdf3*$^{-/-}$ animals was comparable to that seen in *Pparg*$^{fl/fl}$ *Lyz2-cre* animals, *Gdf3*$^{-/-}$ animals did not display persistent inflammation and delayed

resolution of necrotic and/or phagocytic fibers. This suggested that PPARγ regulated several relevant pathways during regeneration. Notably, a gain of function experiment revealed that exogenous GDF3 could counteract the deleterious effect PPARγ deficiency in macrophages. Our *in vitro* results with BMDM supernatants and myoblasts indicated the presence of a regulatory circuit between macrophages and muscle cells and showed that GDF3 appeared to be an especially robust enhancer of myoblast fusion.

As other cell types are also involved in the regeneration process (Heredia et al., 2013; Joe et al., 2010; Uezumi et al., 2010), it cannot be excluded that GDF3 is only one of the TGF-β family members that are active during regeneration and that it has effects on other cell types such as FAPs as well. It is remarkable, though, that the key elements of the myogenic cross talk between cell types can be modeled *in vitro* using macrophages and myoblasts only, arguing that these two cell types and their interactions are critical to support regeneration.

Our findings also carry potential implications for pathological circumstances in which recurrent muscle damage and asynchrony in repair due to genetic conditions leads to debilitating degenerative muscle diseases, such as Duchenne Muscular Dystrophy (DMD). It is of great importance to determine if GDF3 is also a regulator of muscle regeneration in DMD or other types of myopathies, which are most of the time associated with the permanent presence of inflammatory cells, especially macrophages.

MATERIALS AND METHODS

For more detailed descriptions of experimental procedures, please see supplemental materials and methods.

Mice

Pparg$^{fl/fl}$*Lyz2-cre*$^{+}$ and wild type C57BL/6J controls, *Pparg*$^{fl/-}$*Sox2-cre*$^{+}$ and littermate control *Pparg*$^{fl/+}$*Lyz2-cre*$^{-}$ animals, and *Gdf3*$^{-/-}$ and littermate C57BL/6 albino controls were used in the experiments. All experimental procedure conducted on animals were carried out in accordance with institutional regulations.

Muscle injury—Mice were anaesthetized with isoflurane and 50 μl of cardiotoxin (12×10^{-6} mol/l in PBS) was injected in the *tibialis anterior* (TA) muscle. Muscles were recovered for flow cytometry analysis at day 1, 2 or 4 post-injury or for muscle histology at day 8 post-injury.

Histological analysis of muscle regeneration—Muscles were removed and snap frozen in nitrogen-chilled isopentane (−160°C). 8 μm thick cryosections were cut and stained with hematoxylin-eosin (HE). HE stained sections were analyzed for cross sectional area (CSA) or for the presence of phagocytic fibers. Day 8 post CTX slides were also IF stained for Desmin / F4/80 / DAPI.

Macrophage cell culture for conditioned medium generation—Macrophages were obtained from bone marrow (BM) precursor cells that were were cultured in DMEM medium containing 20% FBS and 30% conditioned medium of L929 cell line (enriched in

CSF-1) for 7 days. Macrophages were activated with IFN-γ (50 ng/ml) or IL-4 (10 ng/ml) to obtain macrophage-conditioned medium.

Myogenic precursor cell (MPC) culture—Murine MPCs were obtained from TA muscle and cultured using standard conditions in DMEM/ F12 (Gibco Life Technologies) containing 20% FBS and 2% Ultroser G (Pall Inc). For proliferation studies, MPCs were incubated for 1 day with conditioned medium + 2.5% FBS or with 2.5% FBS medium containing GDF3 mouse recombinant protein. Cells were then incubated with anti-ki67 antibodies (15580 Abcam), which were subsequently visualized using cy3-conjugated secondary antibodies (Jackson Immunoresearch Inc). For differentiation studies, MPCs were incubated for 3 days with conditioned medium containing 2% horse serum or with 2% horse serum medium containing GDF3. Cells were then incubated with anti-desmin antibodies (32362 Abcam), in combination with a cy3-conjugated secondary antibody (Jackson Immunoresearch Inc).

Phagocytosis assay—BMDM cells and C2C12 cells were stained with CellVue or PKH67 (Sigma), respectively. Heat killed stained C2C12 were used as phagocytic substrates for stained BMDMs and fluorescent intensity was measured with a FACScalibur instrument.

Image capture and analysis for myoblast cultures—Fusion index (for myogenic cells) was calculated as the number of nuclei within myotubes divided by the total number of nuclei, nuclei number being estimated using the Image J software.

Isolation of macrophages from muscle—CD45$^+$ cells were isolated from CTX injected muscles using magnetic sorting (Miltenyi Biotec). CD45$^+$ cells then were labeled with fluorescently labeled antibodies and Ly6C$^+$ F4/80^{low} macrophages, Ly6C$^-$ F4/80$^+$ macrophages and Ly6C^{mid} F4/80$^-$ neutrophils were analyzed and sorted with a BD FACSAria III sorter.

RNA isolation from sorted MFs—Macrophage subsets were sorted from day 1, 2 and 4 post-injury muscles with a FACSAria III sorter and total RNA was isolated with TRIZOL reagent according to the manufacturer's recommendation.

Microarray analysis of muscle macrophages—Global expression pattern was analyzed on Affymetrix GeneChip Mouse Gene 1.0 ST arrays. The microarray data are publicly available (Data access: GSE71155).

ChIP (Chromatin immunoprecipitation)—ChIP was carried out in BMDMs using antibodies against pre-immune IgG (Millipore, 12-370), (pan) RXR (sc-774 Santa Cruz Biotechnology) and PPARγ (Perseus #PP-A3409A).

Bioinformatic analysis of the active enhancers around the *Gdf3* and *Angptl4* locus—The list of published and/or publicly available datasets used for visualization in IGV2 to identify active enhancers can be found in the supplemental method section.

Western Blotting—GDF3 protein expression was measured using Western Blot analysis. Samples from CTX injected TA muscles or CD45^{+} cells were lysed in RIPA buffer. GDF3 was targeted using rabbit monoclonal Anti-GDF3 primary antibody (ab109617, Abcam, Cambridge, MA) at 1:1,000 dilution in TBS-T supplemented with 5% BSA overnight at 4°C. Anti-GAPDH mouse monoclonal primary antibody (AM4300, Ambion, Carlsbad, CA) was used as a protein loading control at 1:10,000 – 1:20,000 dilution in TBS-T supplemented with 5% BSA overnight at 4°C.

RNA sequencing (RNA-Seq) library preparation for myoblast gene expression analysis—cDNA library for RNA-Seq was generated from 1μg total RNA using TruSeq RNA Sample Preparation Kit (Illumina, San Diego, CA, USA) according to the manufacturer's protocol.

The RNA-Seq data are publicly accessible (data access: PRJNA290560/SRR2136645).

General statistical analyses—All experiments were performed using at least three different samples. Student's t-tests and 2 way ANOVA analyses were performed and P<0.05 was considered significant (P 0.05=*, P 0.01=**, P 0.0001=***, P 0.001=****). Mean and SD values, or mean and SEM values are shown in graphs.

Supplementary Material

Refer to Web version on PubMed Central for supplementary material.

ACKNOWLEDGEMENTS

REFERENCES

Chazaud B. Macrophages: supportive cells for tissue repair and regeneration. Immunobiology. 2014; 219:172–178. [PubMed: 24080029]

Clausen BE, Burkhardt C, Reith W, Renkawitz R, Forster I. Conditional gene targeting in macrophages and granulocytes using LysMcre mice. Transgenic research. 1999; 8:265–277. [PubMed: 10621974]

Daniel B, Nagy G, Hah N, Horvath A, Czimmerer Z, Poliska S, Gyuris T, Keirsse J, Gysemans C, Van Ginderachter JA, et al. The active enhancer network operated by liganded RXR supports angiogenic activity in macrophages. Genes & development. 2014; 28:1562–1577. [PubMed: 25030696]

Duffield JS, Forbes SJ, Constandinou CM, Clay S, Partolina M, Vuthoori S, Wu S, Lang R, Iredale JP. Selective depletion of macrophages reveals distinct, opposing roles during liver injury and repair. The Journal of clinical investigation. 2005; 115:56–65. [PubMed: 15630444]

Egerman MA, Cadena SM, Gilbert JA, Meyer A, Nelson HN, Swalley SE, Mallozzi C, Jacobi C, Jennings LL, Clay I, et al. GDF11 Increases with Age and Inhibits Skeletal Muscle Regeneration. Cell metabolism. 2015; 22:164–174. [PubMed: 26001423]

Heredia JE, Mukundan L, Chen FM, Mueller AA, Deo RC, Locksley RM, Rando TA, Chawla A. Type 2 innate signals stimulate fibro/adipogenic progenitors to facilitate muscle regeneration. Cell. 2013; 153:376–388. [PubMed: 23582327]

Huang JT, Welch JS, Ricote M, Binder CJ, Willson TM, Kelly C, Witztum JL, Funk CD, Conrad D, Glass CK. Interleukin-4-dependent production of PPAR-gamma ligands in macrophages by 12/15-lipoxygenase. Nature. 1999; 400:378–382. [PubMed: 10432118]

Jiang C, Wang JH, Yue F, Kuang S. The brain expressed x-linked gene 1 (Bex1) regulates myoblast fusion. Developmental biology. 2016; 409:16–25. [PubMed: 26586200]

Joe AW, Yi L, Natarajan A, Le Grand F, So L, Wang J, Rudnicki MA, Rossi FM. Muscle injury activates resident fibro/adipogenic progenitors that facilitate myogenesis. Nature cell biology. 2010; 12:153–163. [PubMed: 20081841]

Koo JH, Smiley MA, Lovering RM, Margolis FL. Bex1 knock out mice show altered skeletal muscle regeneration. Biochemical and biophysical research communications. 2007; 363:405–410. [PubMed: 17884015]

Laflamme MA, Murry CE. Heart regeneration. Nature. 2011; 473:326–335. [PubMed: 21593865]

Lemos DR, Babaeijandaghi F, Low M, Chang CK, Lee ST, Fiore D, Zhang RH, Natarajan A, Nedospasov SA, Rossi FM. Nilotinib reduces muscle fibrosis in chronic muscle injury by promoting TNF-mediated apoptosis of fibro/adipogenic progenitors. Nature medicine. 2015; 21:786–794.

Levine AJ, Brivanlou AH. GDF3, a BMP inhibitor, regulates cell fate in stem cells and early embryos. Development. 2006; 133:209–216. [PubMed: 16339188]

Levine AJ, Levine ZJ, Brivanlou AH. GDF3 is a BMP inhibitor that can activate Nodal signaling only at very high doses. Developmental biology. 2009; 325:43–48. [PubMed: 18823971]

Matsumura K, Tome FM, Collin H, Azibi K, Chaouch M, Kaplan JC, Fardeau M, Campbell KP. Deficiency of the 50K dystrophin-associated glycoprotein in severe childhood autosomal recessive muscular dystrophy. Nature. 1992; 359:320–322. [PubMed: 1406935]

McPherron AC, Lawler AM, Lee SJ. Regulation of skeletal muscle mass in mice by a new TGF-beta superfamily member. Nature. 1997; 387:83–90. [PubMed: 9139826]

Merkenschlager M, Odom DT. CTCF and cohesin: linking gene regulatory elements with their targets. Cell. 2013; 152:1285–1297. [PubMed: 23498937]

Mounier R, Theret M, Arnold L, Cuvellier S, Bultot L, Goransson O, Sanz N, Ferry A, Sakamoto K, Foretz M, et al. AMPKalpha1 regulates macrophage skewing at the time of resolution of inflammation during skeletal muscle regeneration. Cell metabolism. 2013; 18:251–264. [PubMed: 23931756]

Nadra K, Quignodon L, Sardella C, Joye E, Mucciolo A, Chrast R, Desvergne B. PPARgamma in placental angiogenesis. Endocrinology. 2010; 151:4969–4981. [PubMed: 20810566]

Odegaard JI, Ricardo-Gonzalez RR, Goforth MH, Morel CR, Subramanian V, Mukundan L, Red Eagle A, Vats D, Brombacher F, Ferrante AW, et al. Macrophage-specific PPARgamma controls alternative activation and improves insulin resistance. Nature. 2007; 447:1116–1120. [PubMed: 17515919]

Rapalino O, Lazarov-Spiegler O, Agranov E, Velan GJ, Yoles E, Fraidakis M, Solomon A, Gepstein R, Katz A, Belkin M, et al. Implantation of stimulated homologous macrophages results in partial recovery of paraplegic rats. Nature medicine. 1998; 4:814–821.

Shen JJ, Huang L, Li L, Jorgez C, Matzuk MM, Brown CW. Deficiency of growth differentiation factor 3 protects against diet-induced obesity by selectively acting on white adipose. Molecular endocrinology. 2009; 23:113–123. [PubMed: 19008465]

Szanto A, Balint BL, Nagy ZS, Barta E, Dezso B, Pap A, Szeles L, Poliska S, Oros M, Evans RM, et al. STAT6 transcription factor is a facilitator of the nuclear receptor PPARgamma-regulated gene expression in macrophages and dendritic cells. Immunity. 2010; 33:699–712. [PubMed: 21093321]

Tonkin J, Temmerman L, Sampson RD, Gallego-Colon E, Barberi L, Bilbao D, Schneider MD, Musaro A, Rosenthal N. Monocyte/Macrophage-derived IGF-1 Orchestrates Murine Skeletal Muscle Regeneration and Modulates Autocrine Polarization. Molecular therapy : the journal of the American Society of Gene Therapy. 2015; 23:1189–1200. [PubMed: 25896247]

Tontonoz P, Nagy L, Alvarez JG, Thomazy VA, Evans RM. PPARgamma promotes monocyte/macrophage differentiation and uptake of oxidized LDL. Cell. 1998; 93:241–252. [PubMed: 9568716]

Uezumi A, Fukada S, Yamamoto N, Takeda S, Tsuchida K. Mesenchymal progenitors distinct from satellite cells contribute to ectopic fat cell formation in skeletal muscle. Nature cell biology. 2010; 12:143–152. [PubMed: 20081842]

Varga T, Mounier R, Gogolak P, Poliska S, Chazaud B, Nagy L. Tissue LyC6-macrophages are generated in the absence of circulating LyC6-monocytes and Nur77 in a model of muscle regeneration. Journal of immunology. 2013; 191:5695–5701.

Varga T, Mounier R, Horvath A, Cuvellier S, Dumont F, Poliska S, Ardjoune H, Juban G, Nagy L, Chazaud B. Highly Dynamic Transcriptional Signature of Distinct Macrophage Subsets during Sterile Inflammation, Resolution, and Tissue Repair. Journal of immunology. 2016; 196:4771–4782.

Welch JS, Ricote M, Akiyama TE, Gonzalez FJ, Glass CK. PPARgamma and PPARdelta negatively regulate specific subsets of lipopolysaccharide and IFN-gamma target genes in macrophages. Proceedings of the National Academy of Sciences of the United States of America. 2003; 100:6712–6717. [PubMed: 12740443]

HIGHLIGHTS

➢ Macrophage PPARγ is required for skeletal muscle regeneration

➢ PPARγ regulates GDF3 in muscle infiltrating LyC6⁻ repair macrophages

➢ The *Gdf3* locus has multiple PPARγ:RXR heterodimer bound active enhancers

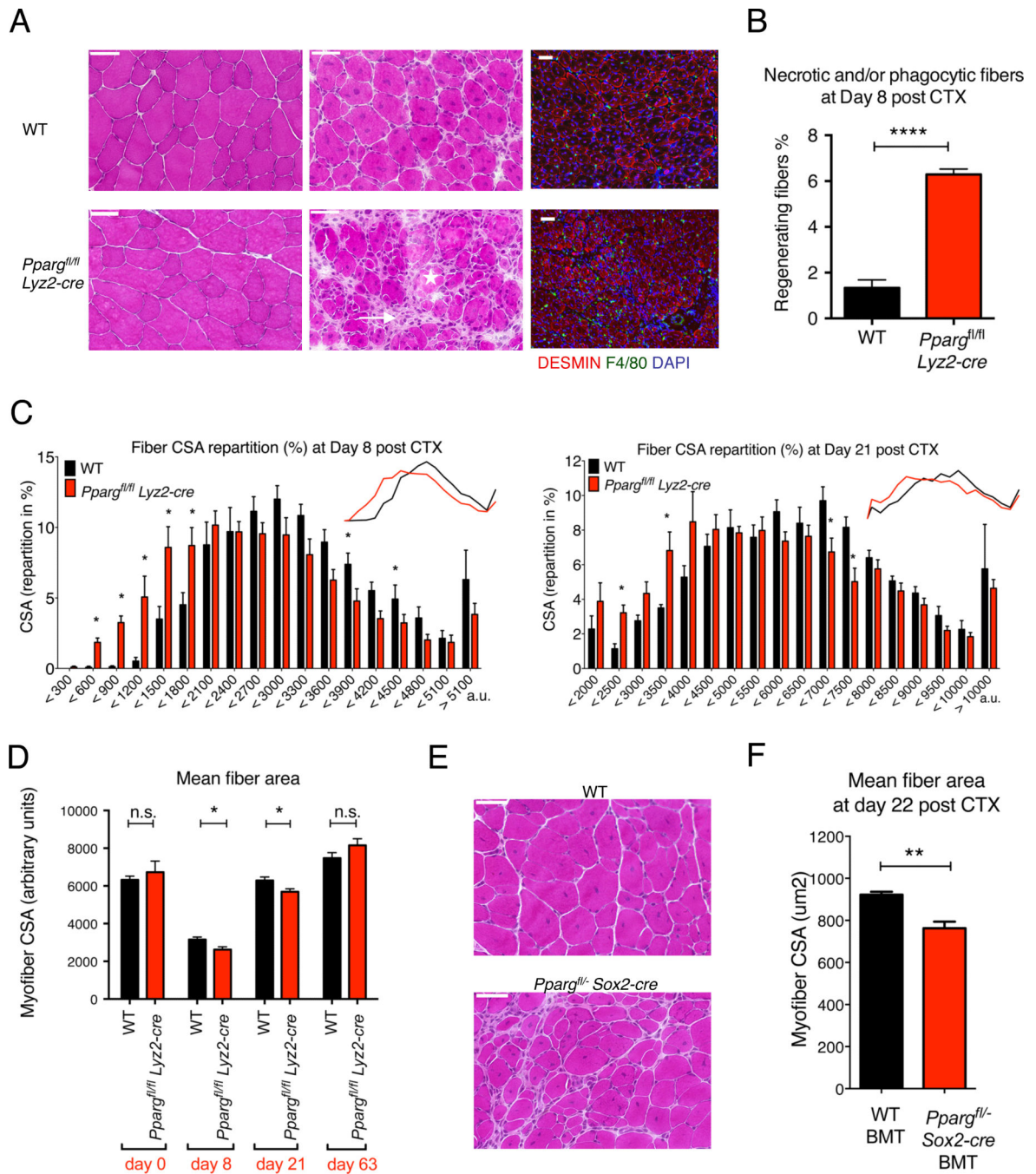➢ GDF3 regulates muscle regeneration and enhances primary myoblast fusion

Fig 1. Impaired regeneration of skeletal muscle in PPARγ deficient animals

(A) Representative images of HE stained skeletal muscle from WT and *Pparg*^{fl/fl} *Lyz2-cre* animals prior (day 0) or post CTX induced injury (day 8) are shown. Asterisk labels phagocytic and/or necrotic fibers and arrow points to foci of inflammatory infiltrations. IHC detection of desmin (red), F4/80 (green) and nuclei (blue) at day 8 post CTX injury is also shown. Scale bars in the upper left represent 50 μm. (B) The ratio of phagocytic and/or necrotic fibers relative to all regenerative fibers at day 8 of regeneration in WT and *Pparg*^{fl/fl} *Lyz2-cre* muscle sections is shown. (C) Fiber size repartition of regenerating muscle in WT

or *Pparg*^{fl/fl} *Lyz2-cre* animals at day 8 and day 21 post CTX injury. (D) Average fiber cross section area (CSA) of regenerating muscle at indicated timepoints post CTX injury in WT and *Pparg*^{fl/fl} *Lyz2-cre* animals. (E) Representative images of HE stained skeletal muscle 22 days after CTX injury from bone marrow transplanted (BMT) animals that received either WT or *Pparg*^{fl/−} *Sox2-cre* bone marrow. n=4 or 4, 5 or 6, 5 or 5 and 5 or 5 muscles for WT or *Pparg*^{fl/fl} *Lyz2-cre* mice, respectively, at day 0, 8, 21 and 63. (F) Muscle fiber CSA of BMT animals 22 days post CTX injury. n= 8 muscles for both genotypes. In all bar graphs, mean values +/− SEM are shown. For *Pparg* expression in macrophages and CD45$^+$ cells and for additional histological analysis, see Fig S1 and S2. For the FACS analyses of infiltrating cells see Fig S3.
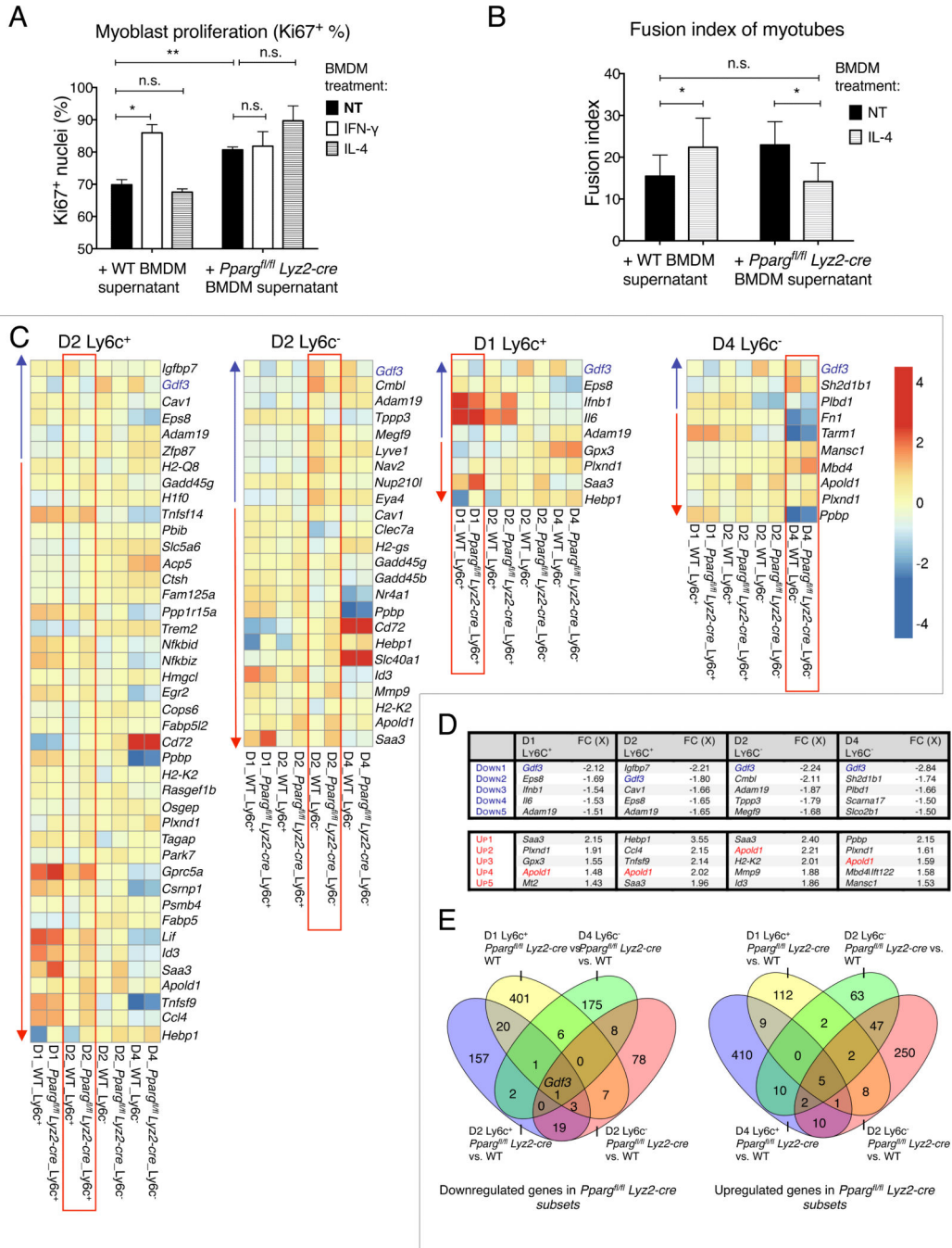
Fig 2. PPARγ regulated macrophage functions and genes

(A) Effect of BMDM derived conditioned media on the proliferation of primary myoblasts
(+/− SEM). n= 4 or 3 for WT or *Pparg*fl/fl *Lyz2-cre* BMDM supernatant. (B) Effect of
BMDM derived conditioned media on the differentiation of primary myotubes (+/− SEM).
For the complete analysis, see Figs S4C-D. n=6 for both genotypes. (C-E) Transcriptional
analysis of the Ly6C+ and Ly6C− macrophage populations derived from WT and *Pparg*fl/fl
Lyz2-cre animals. For schematics of comparisons, see Fig S4F. (C) Heatmap representation
of genes that show differential (p=0.05, min. 1.5X FC) expression in the four sorted WT *vs.*

Pparg^{fl/fl} *Lyz2-cre* macrophages in day 1 Ly6C$^+$, D2 Ly6C$^+$ and D2 Ly6C$^-$, and D4 Ly6C$^-$ cells (labeled as D1 Ly6C$^+$ etc.). In each heatmap, the differentially expressed genes are highlighted within a red square and the expression pattern of these genes in the other macrophage subtypes is also shown for reference. Blue and red arrows label genes that are downregulated or upregulated in WT *vs. Pparg*^{fl/fl} *Lyz2-cre* cells, respectively. The blue and red arrows point to the direction of increasing fold change difference. For RT-qPCR validation of mRNA expression, see Fig S5. (D) Top 5 up and downregulated genes in the four sorted macrophage populations in *Pparg*^{fl/fl} *Lyz2-cre* macrophages. Table lists gene symbols and fold change differences (FC). *Gdf3* and *Apold1*, the genes that are down-, or upregulated in *Pparg*^{fl/fl} *Lyz2-cre* in all four subtypes, are highlighted in color. (E) Venn-diagrams show the overlap of the number of genes that are down-, or upregulated in *Pparg*^{fl/fl} *Lyz2-cre* macrophages in the four analyzed populations.
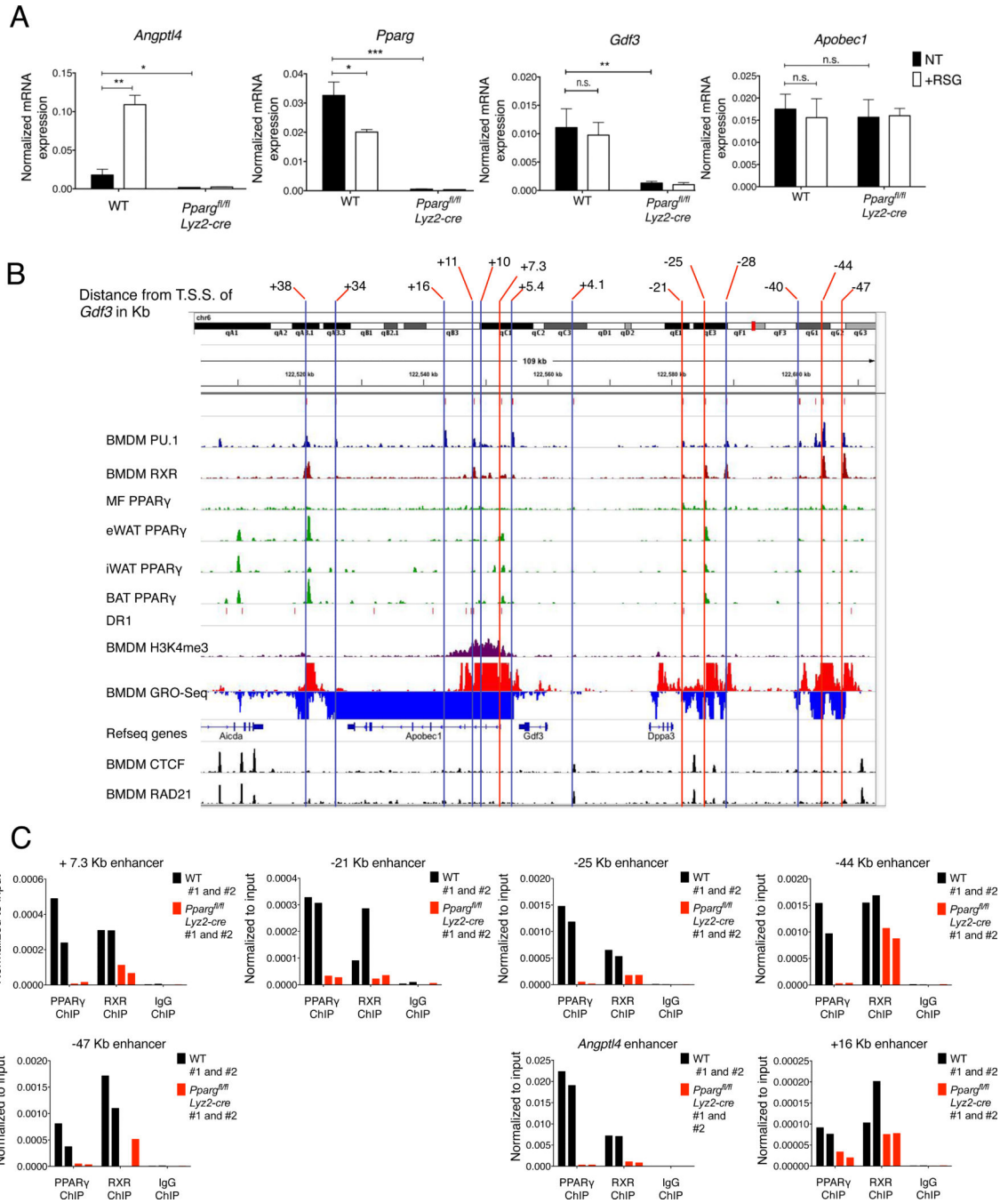
Fig 3. *Gdf3* is a PPARγ target gene in BMDMs

(A) mRNA expression of *Angptl4*, a canonical PPARγ target gene, *Pparg*, *Gdf3* and *Apobec1*, a nearby, not regulated gene, are shown in BMDMs (n=4 for WT and n=5 for *Pparg*fl/fl *Lyz2-cre*). (B) Identification of possible enhancers around the *Gdf3* locus. The selection criteria for enhancers possibly involved in *Gdf3* regulation are described in the text and in Figs S6A-B. Putative enhancers are labeled by vertical lines. Blue verticals highlight enhancers without PPARγ ChIP enrichment, red verticals label enhancers where enrichment in PPARγ binding in WT BMDMs was detected by PPARγ ChIP. (C) ChIP on the putative

enhancer regions reveal PPARγ binding at +7.3 Kb, −21 Kb, −25 Kb, −44 Kb and −47 Kb enhancers around the *Gdf3* locus. Representative graphs showing PPARγ, RXR or IgG ChIPs carried out on 2 samples are shown. *Angptl4* enhancer and *Gdf3* +16 kB enhancer are shown as positive and negative controls, respectively.
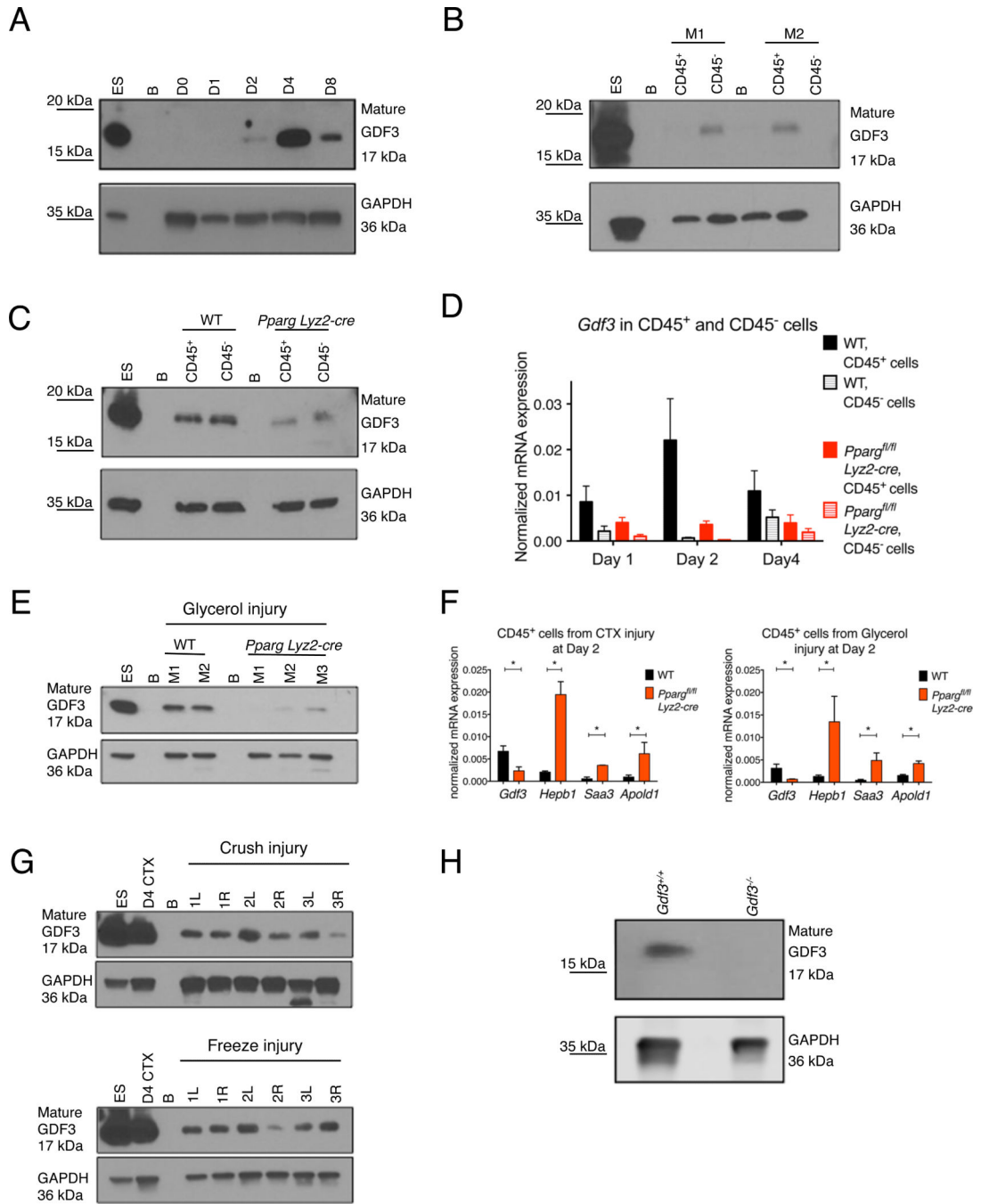
Fig. 4. GDF3 mRNA and protein expression in regenerating muscles

ES and B stand for embryonic stem cells and blank, respectively. (A) GDF3 protein expression in whole muscle lysates of regenerating muscles from WT mice at different timepoints (D=day). (B) GDF3 mRNA expression in CD45$^+$ and CD45$^−$ cells isolated at day 4 post CTX injury from WT and *Pparg*$^{fl/fl}$ *Lyz2-cre* mice (M=mouse). (C) Decreased protein expression of GDF3 in CD45$^+$ cells isolated from *Pparg*$^{fl/fl}$ *Lyz2-cre* animals. (D) mRNA expression of *Gdf3* in CD45$^+$ and CD45$^−$ cells isolated from injured muscles at days 1, 2 and 4 post CTX in WT and *Pparg*$^{fl/fl}$ *Lyz2-cre* animals. n=4 for each day, cell type and

genotype. (E) GDF3 protein expression detected in muscles lysates generated from glycerol mediated injuries (M=mouse). (F) Concordant mRNA expression pattern of PPARγ-dependent genes in CTX and Glycerol mediated injuries. n=3 for both treatments. (G) GDF3 protein expression detected in muscle lysates generated from crush or freeze injuries (R and L stand for right and left leg, respectively). (H) Specificity of the anti-GDF3 antibody is demonstrated in day 4 CTX injured WT and *Gdf3*$^{-/-}$ muscle samples.
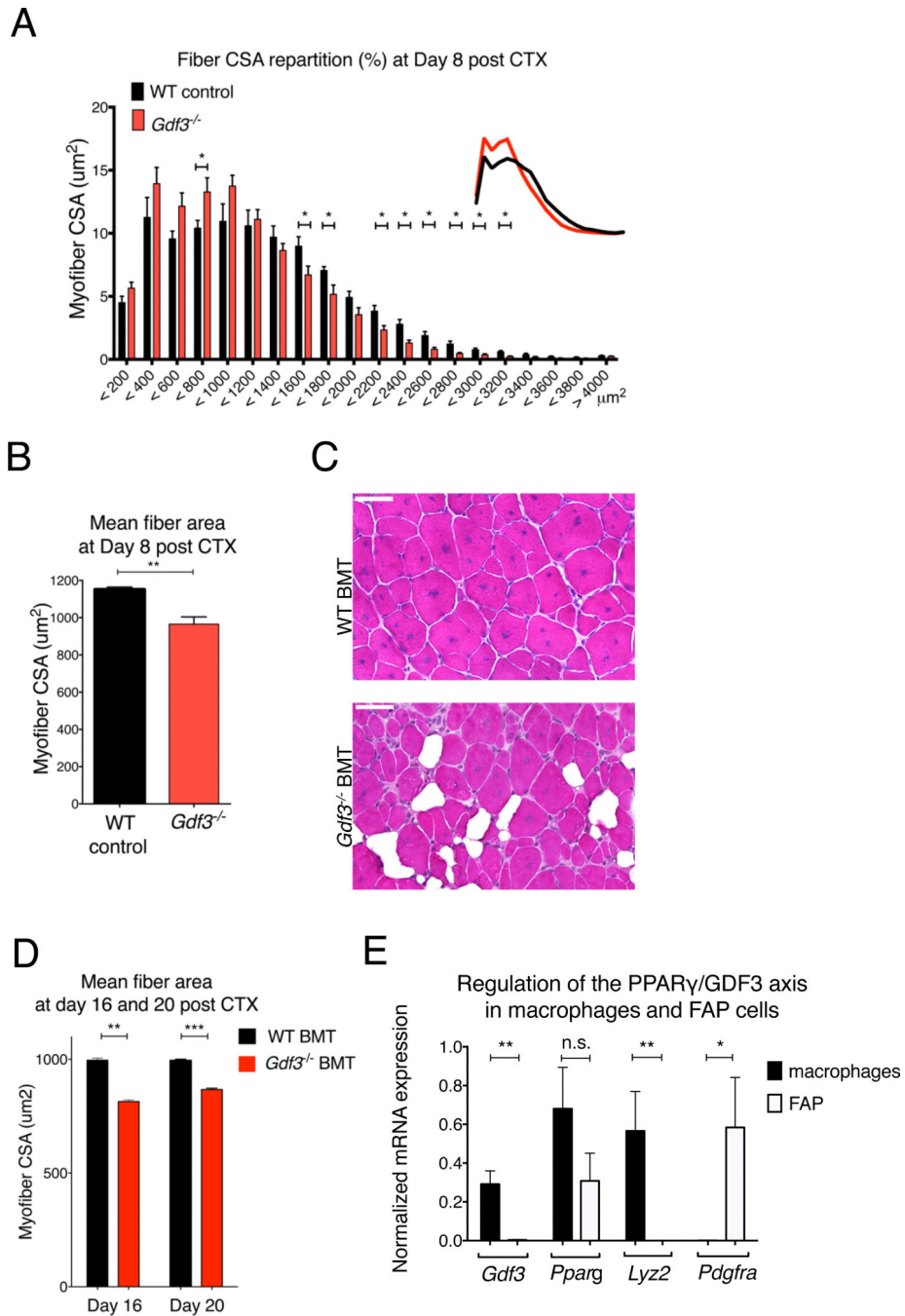
Fig 5. GDF3 deficiency impairs muscle regeneration

(A, B) Myofiber CSA repartition (A) and mean CSA (B) in CTX injured WT or $Gdf3^{-/-}$ muscles at day 8. N=7 or 7 muscles for WT or $Gdf3^{-/-}$ mice. (C) Representative HE stained muscle sections of WT BMT and $Gdf3^{-/-}$ BMT animals, 16 days post CTX injury. Scale bars represent 50 μm. n= 4 muscles for both timepoints and genotypes. (D) Myofiber CSA measurement in WT BMT and $Gdf3^{-/-}$ KO BMT animals, 16 and 20 days post CTX injury. (E) Lack of $Gdf3$ and $Lyz2$ mRNA expression in PDGFRA[+] FAPs isolated from regenerating muscle at day 2 post-injury n=3.
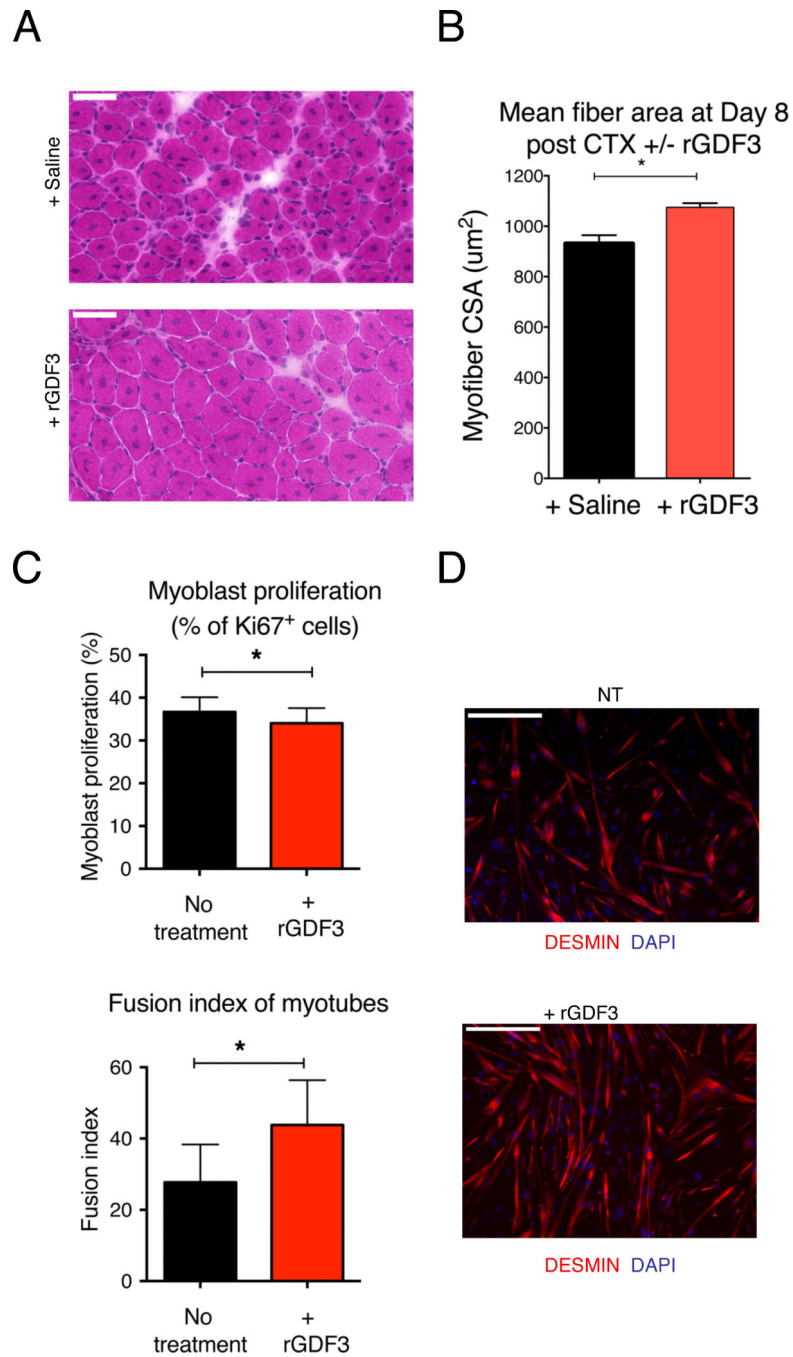
Fig 6. Effects of recombinant GDF3 on muscle differentiation
(A, B) Improvement in regeneration by administration of recombinant GDF3 in *Pparg*fl/fl *Lyz2-cre* animals. (A) HE stained images and (B) CSA measurements are shown. (C) In vitro proliferation and differentiation assays on primary myoblasts in the presence of recombinant GDF3. n=4. (D) IF against Desmin (red) and DAPI (blue) shows a drastic enhancement of myotube formation in the presence of recombinant (r) GDF3 in the *in vitro* primary myoblast myogenesis assay n=3. In all bar graphs, bars represent mean +/− SEM.

For the effect of rGDF3 on myogenic differentiation and fusion, see Fig S7. Scale bars represent 50 μm in each image in Fig. 6A and D.
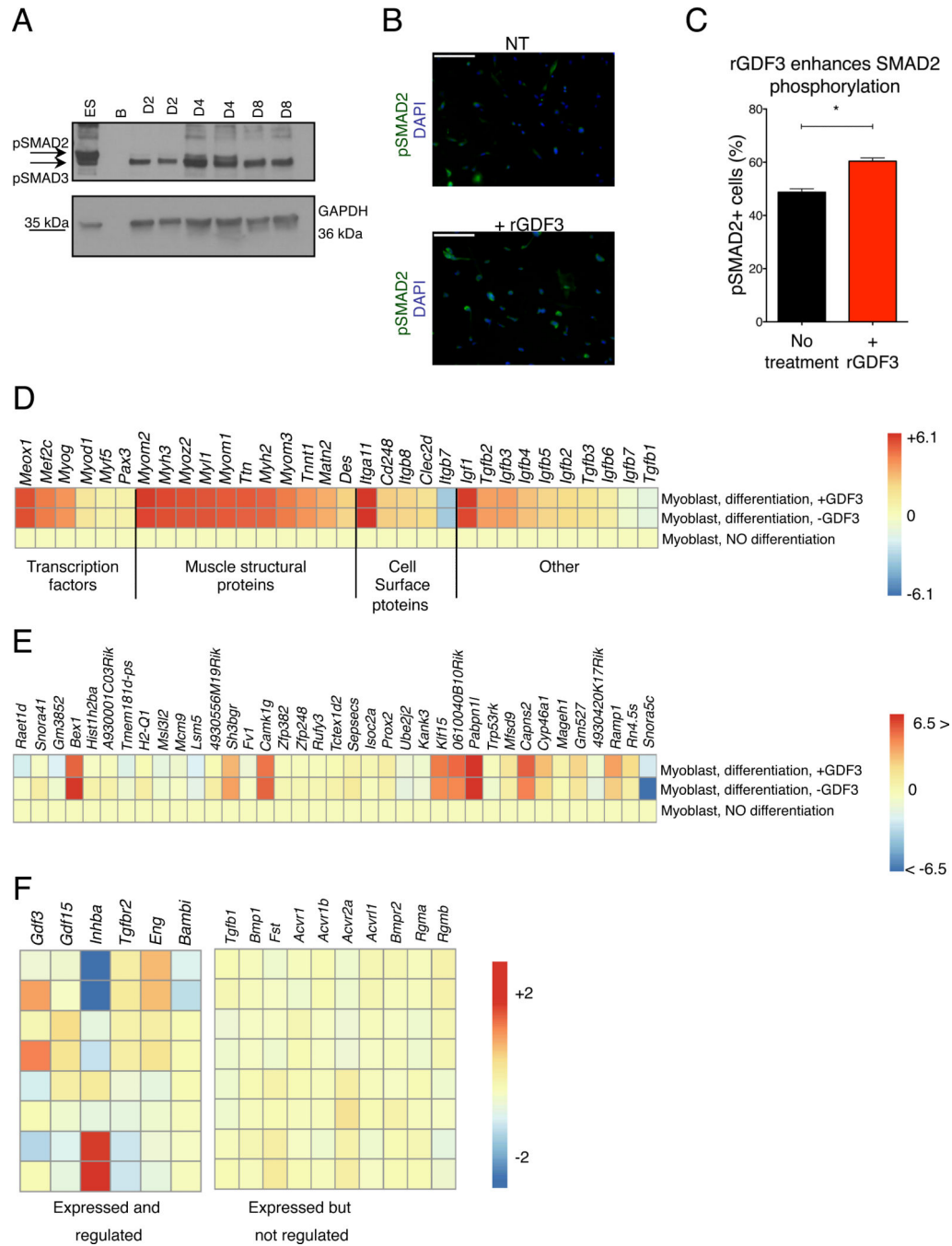
Fig 7. Effects of GDF3 on myogenesis

(A) Increased pSmad2 phosphorylation in regenerating muscles peaking at day 4 post CTX injury. (B-C) Increased Smad2 phosphorylation in primary myoblasts treated with rGDF3. IF images and % of pSMAD2 positive cells are shown. n=3. (D) Heatmap representation of the expression changes of myogenic genes validating the utilized *in vitro* primary myoblast assay. (E) Heatmap representation of genes that are differentially expressed (min. fold change difference of 1.2X between differentiated myoblasts +/− rGDF3) in the presence of recombinant GDF3 during myoblast differentiation. (F) Heatmap representation of members

of the TGF-β superfamily signaling system that are expressed and regulated, or expressed but not regulated in muscle derived macrophages. For non-expressed members, see Fig S7C.